Electronic Supplementary Material (ESI) for ChemComm.

Supporting Information

Unexpected Functions of Oxygen in Chemical Vapor Deposition Atmosphere to Regulate Graphene Growth Modes

Jing Li, [a,b] Dong Wang*[a] and Li-Jun Wan*[a]

[a] CAS Key Laboratory of Molecular Nanostructure and Nanotechnology and Beijing National Laboratory for Molecular Sciences, Institute of Chemistry, Chinese Academy of Sciences (CAS), Beijing 100190, P. R. China

[b] University of Chinese Academy of Sciences, Beijing 100049, P. R. China.

E-mail: wangd@iccas.ac.cn; wanlijun@iccas.ac.cn.

Materials and graphene growth.

Graphene films were grown on 25 μm thick Cu foils (Alfa Aesar, item no. 13382) at 1070 ˚C in a one-inch corundum tube furnace at atmospheric pressure. Before the graphene growth process, the CVD chamber was pumped to 0.1 Pa, and then 500 sccm Ar flow was used to flush the CVD chamber for 1 minute. After pumped and flushed for three times, the CVD chamber was adjusted to atmospheric pressure for graphene growth. The pre-cleaned[1] Cu foils were first heated and annealed at 1050 ˚C for 30 min under 450 standard cubic centimeters per minute (sccm) Ar and 50 sccm H_2, and then 100 sccm mixture gas containing 5 sccm diluted methane (500 ppm in Ar), 2.5 sccm H_2, diluted oxygen (50 or 500 ppm in Ar) and Ar was applied for graphene growth. All the gases are of ultrahigh purity (with the purity of 99.999% purity) and purchased from Tailong Electronics. The oxygen concentration was measured by the gas analysis (DF-OMT, DFAI Nanjing). The oxygen concentration of ultrahigh purity Ar is about 0.8 ppm. After graphene growth at designated time, the samples were rapidly cooled down to room temperature in 30 min for further characterization.

Graphene transfer.

For Raman spectroscopy and AFM characterization, graphene was transferred onto SiO_2 substrate by the wet-transfer method as reported elsewhere.[1] In general, one side of the graphene/copper surface was spin-coated with PMMA (Poly (methyl methacrylate), 950 PMMA A4, MicroChem) and baked at 120 ˚C for 1 min. It is worth mention that the graphene can grow on the both side of Cu foil. To eliminate the morphology influence of graphene from the back side of Cu surface, the back side graphene was removed by O-plasma treatment for tens of seconds to minutes depending on the film thickness. 0.1M $(NH_4)_2S_2O_8$ (Sigma Aldrich) solution was used to etch Cu foil overnight. After washed by deionized water for several times, the PMMA/Graphene film was pick up by target substrate, and dried in vacuum. Finally, the PMMA layer was dissolved in hot acetone for 1 hour.

Characterizations.

The graphene morphology was characterized with field-emission scanning electron microscopy (SEM, JEOL 6701F, 5kV) on Cu. The structure characterization was performed by Raman spectroscopy (Thermo Scientific DXR, 532 nm laser wavelength) on SiO_2/Si substrate. The graphene structure and thickness was studied by scanning probe microscopy [atomic force microscopy (AFM, Veeco Multimode) and scanning tunneling microscopy (STM, Agilent Technologies)]. The surface elemental information was analyzed by the X-ray photoelectron spectroscopy (XPS) on the Thermo Scientific ESCALab 250Xi with 200W Al Kα radiation and Electron Probe Microanalyzer (EPMA, SHIMADZU, EPMA-1720, 15kV).

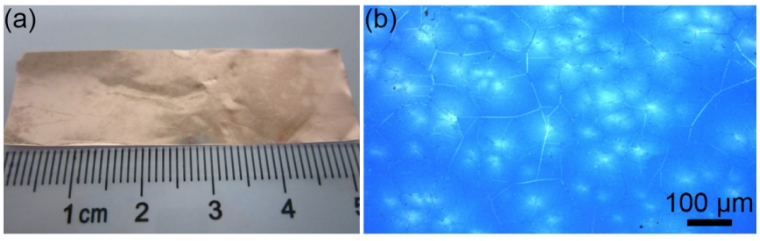

Figure S1. (a) Optical photograph of graphene on Cu foil, which was obtained under the growth atmosphere containing 5 sccm diluted methane (500 ppm in Ar), 2.5 sccm H_2, and 92.5 sccm high purity Ar for 90 h. (b) The correspondent optical microscope image of the graphene in panel (a) that was transferred onto 300 nm SiO_2/Si substrate.

Multilayer graphene formation process.

To have a better demonstration about the multilayer graphene formation process, we present the growth process of multilayer graphene at different growth time at the oxygen concentration of 1.8 ppm in Figure S2. At the growth time of 60 min, (Figure S2a) the hexagonal single layer graphene forms on Cu substrate. After the growth time of 150 min, the graphene film mainly of mono-layer can cover the whole Cu surface with the bi-layer coverage about 15%. With the growth time of 300 min, the bi-layer graphene ratio can be about 60%, and some tri-layer and multilayer (layer number > 5) domains begin to appear. The bi-layer graphene domains can be about 85% at the growth time of 400 min. (Figure S2d) Further increasing the growth time to 600 min, the Cu substrate is covered by thick graphene films beyond 5 layers in most domains. It is worth noting that during all these growth process, the domains of multi-layer graphene keep on extending while with the Cu substrate is fully covered by a graphene film, and no graphene crack or exposed Cu surface were observed by SEM throughout this process. Further increasing the growth time would result in disappearing of multilayer graphene gradually and cracking of graphene film. (Figure S2f) Finally, the multilayer graphene layer disappears and the large size graphene flakes further break into smaller size irregular-edged monolayer graphene fragments.

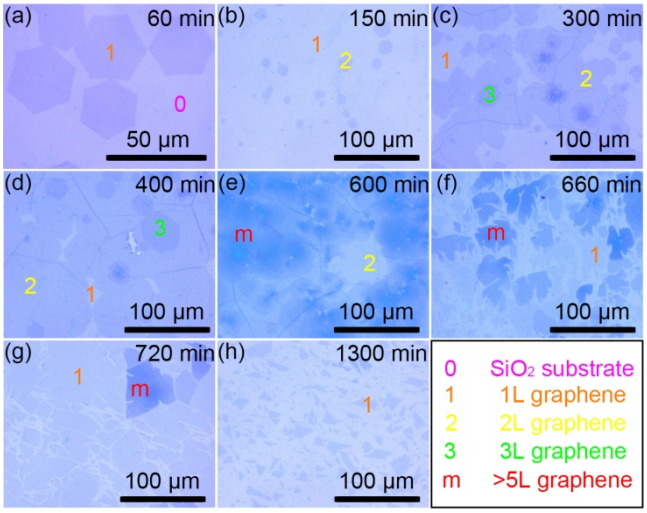

Figure S2. Time-dependent evolution of graphene structure in the growth atmosphere with 1.8 ppm concentration of oxygen in CVD chamber. The growth time is labeled in each image, and the graphene thickness is marked in each image for visual guidance. The correspondent Raman spectroscopies can be found in Figure S3.

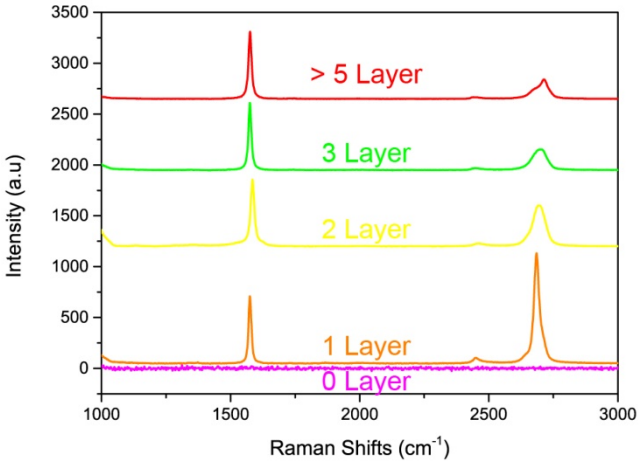

Figure S3. The Raman spectroscopies (all normalized to G peak, around 1580 cm^{-1}) of the graphene as labeled in Figure S2.

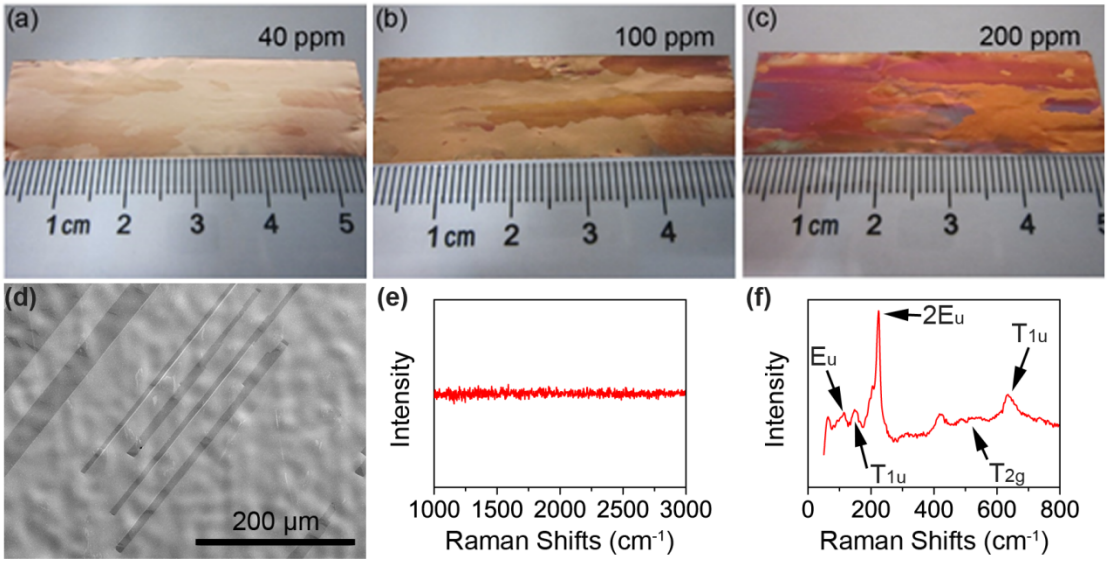

Figure S4. Optical photograph and Raman spectra of Cu foils which were grown under the growth atmosphere containing 40 ppm (a), 100 ppm (b) and 200 ppm (c) extra-introduced oxygen for 240 min, respectively. The SEM image (d) and Raman spectrum (e) indicate no graphene signal on Cu surface of panel (a). The oxidized Cu surface shows the Raman features of Cu_2O (118 cm^{-1}, 149 cm^{-1}, 222 cm^{-1}, 633cm^{-1}),[2, 3] and the typical Raman spectrum of the oxidized Cu surface in panel (a) is revealed in panel (f).

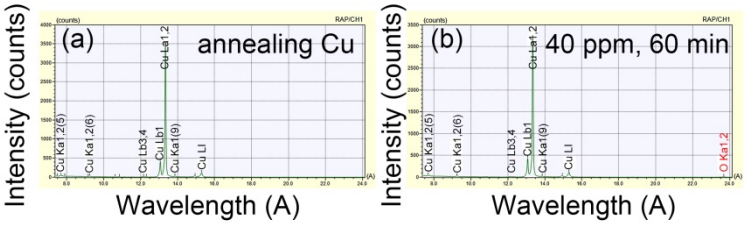

Figure S5. EPMA analysis of the Cu foil surface, which was annealed at 1050 ˚C in 450 sccm Ar and 50 sccm H_2 for 25 min (a), and annealed in the CVD atmosphere (containing 2.5 sccm H_2, 80 sccm diluted oxygen (50 ppm in Ar) and 17.5 sccm Ar) for 60 min.(b) The EPMA results further reveals the formation of Cu_2O in the CVD atmosphere containing ppm grade of oxygen.

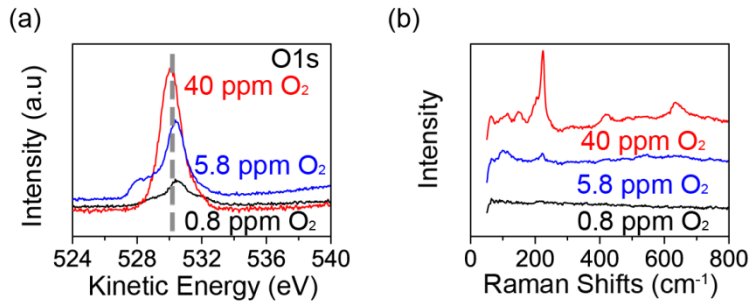

Figure S6. XPS (a) and Raman (b) analysis of the Cu foil surface, which was treated at 1070 ˚C for 60 min in the CVD atmosphere but without CH_4 (containing 2.5 sccm H_2, diluted oxygen and Ar without CH_4) for 60 min. The XPS and Raman results confirm the formation of Cu_2O in the CVD atmosphere containing ppm grade of oxygen.

Some other possible influence factors on multi-layer graphene growth morphology.

Due to the variable external electric field tuned band gap structure of Bernal-stacking bilayer graphene, great efforts have been devoted to grow graphene of multilayer. Generally speaking, the growth temperature,[1, 4] pressure,[5-7] substrate solubility of carbon[8, 9] and penetration effect[10-12] are the main influence factors for multi-layer graphene formation. To further identify the origin of carbon source for multilayer graphene growth, some control experiments were carried out. Considering the growth temperature and pressure are stable during all the graphene growth process, the carbon source for multilayer graphene growth should come from either the substrate or the penetration through the uplayer graphene.

The purity and thickness of Cu substrate.

The Cu foils used in our series of experiments are of 99.8% purity (Alfa Aesar, item no. 13382, 25μm thick). To study the effect of the 0.2% impurity on the graphene growth morphology, we choose the Cu foil of 99.999% purity (Alfa Aesar, item no.10950, 25μm thick) for graphene growth with the same growth parameters as that of 99.8% purity Cu foil. The optical photographs of graphene in Figure S7 show little difference in graphene morphology and thickness with that grown on 99.8% purity Cu foil. Thus the 0.2 % impurity in Cu substrate should not be responsible for the multilayer graphene growth.

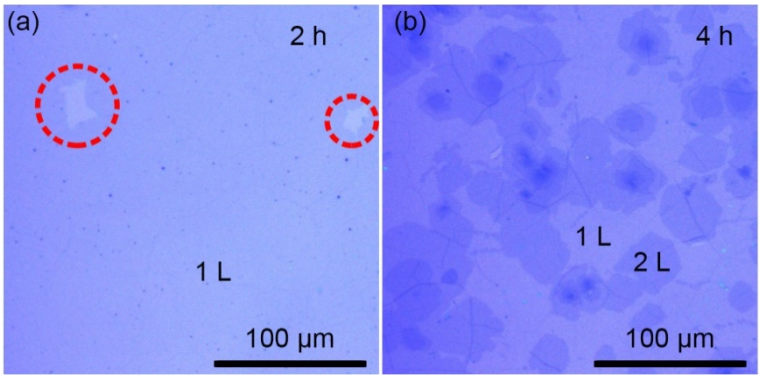

Figure S7. optical microscopy images of graphene which was grown on 99.999% purity Cu foil and transferred onto SiO_2/Si substrate. The growth atmosphere is the same with that of 0.8 ppm oxygen for 99.8% purity Cu foil, and the growth time is labeled in each image. The red dashed circles mark the exposed SiO_2 substrate, and the typical graphene layer-number is marked in each image.

According to the result as reported by Zhao et al, the carbon atoms can penetrate the 25 μm Cu foil within 2.2 s and sustain the multilayer graphene growth on the Cu surface. To confirm whether the carbon atoms for multilayer graphene growth comes from the penetration from the back-side exposed Cu foil, we choose Cu foils of different thickness (Alfa Aesar, item no. 13380, 0.127mm thick; Alfa Aesar, item no. 40374, 0.675mm thick) and observe the graphene morphology on the both side of Cu foil surface. However, the Cu foil thickness turns out to have negligible influence on the multilayer graphene growth. The graphene can fully cover the both Cu surface within 150 min, Further extending growth time results in the growth of multilayer graphene with little morphology difference on the both Cu foil surface. (as shown in Figure S8) Thus the carbon atoms for multilayer graphene growth cannot come from the penetration through the Cu foil from the other surface but highly likely come from the penetration through the graphene film from the CVD atmosphere.

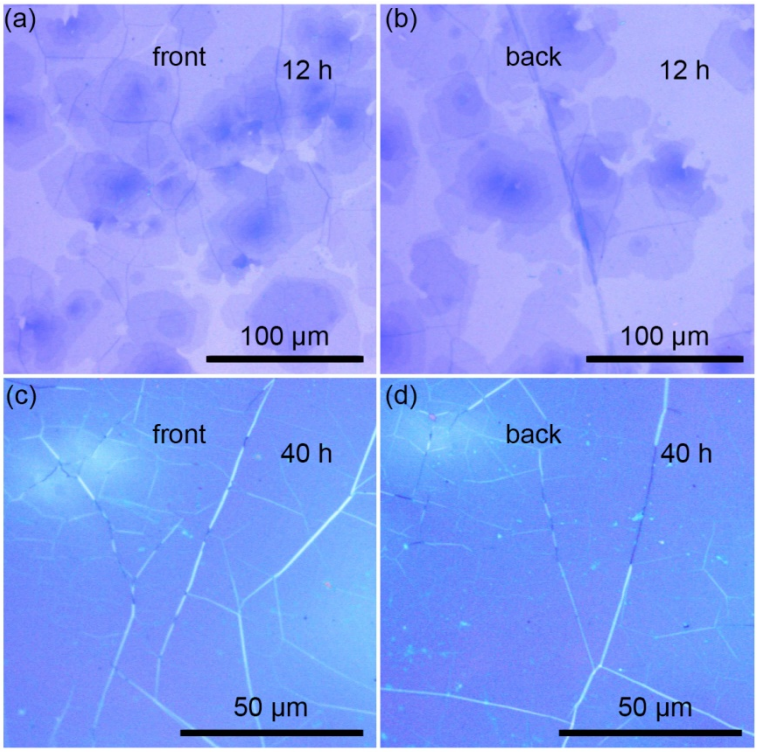

Figure S8. Optical microscopy images of the graphene on SiO_2/Si substrate which was grown on the both sides of 0.675mm thick Cu foil.

XPS characterization of cuprous oxides formation and oxygen intercalation.

XPS was used to characterize the Cu surface composition. As reported previously,[13] the oxygen can penetrate into the space between graphene and Cu substrate in tens of minutes. To minimize the oxygen influence from the air exposure when transferring the graphene sample from CVD chamber to the XPS vacuum chamber, we chose the graphene sample with full coverage on Cu substrate to decrease the oxygen penetration from the graphene fragments edge. Besides, the samples as shown in Figure S9 were sent into the XPS chamber immediately after taken out from the CVD chamber with almost the same exposure time in air less than 5 minutes. The missing of shake up peak between the $2p_{1/2}$ (~932.6 eV) and $2p_{3/2}$ (~952.3eV) peak indicates that the Cu foil is mainly of metal state with minor oxidation of Cu_2O. The m peak (~918.3eV) in panel (b) is correspondent to the feature of metal Cu, and the n peak (916.5eV) is ascribed to the formation of Cu_2O. The variation of n peak intensity proves the Cu substrate oxidation degree is influenced by the oxygen atmosphere in CVD chamber. Besides, the O1s spectrum in panel (c) shows the existence and content difference of Cu_2O (~530.2 eV) between the graphene and Cu foil, which further proves that higher oxygen concentration in CVD chamber can result in higher Cu oxidation degree in the formation of Cu_2O. The peak between 531 to 532 eV in panel (c) should be assigned to the absorbed oxygen on graphene surface.[13] The annealed Cu foil was characterized by XPS for control. (As shown in Figure S9c) The higher peak intensity of Cu_2O (~530.2 eV) is correspondent to the Cu surface oxidation in transferring Cu foil from CVD chamber to XPS chamber without the protection of graphene on the Cu surface.

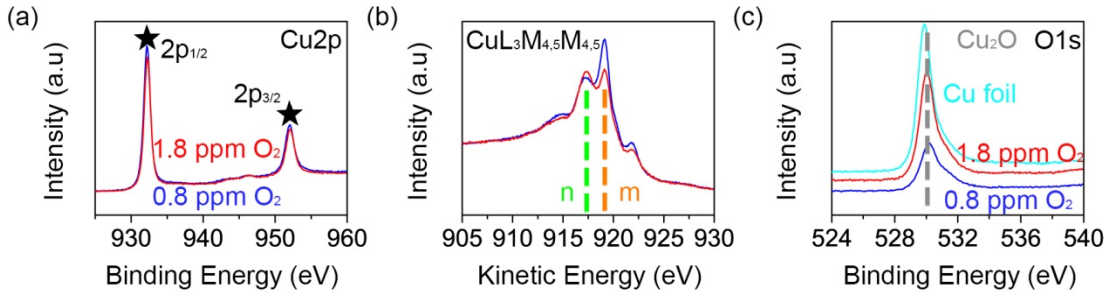

Figure S9. The XPS spectra of Cu2p (a), $CuL_3M_{4,5}M_{4,5}$ Auger (b) and O1s (c) of the graphene sample which was grown in the atmosphere containing 1.8 ppm O_2 (red line) for 4 h and 0.8 ppm O_2 (blue line) for 4 h, respectively.

The formation process of hexagonal graphene fragments.

The SEM observation indicates that the etching process preferentially begins from the graphene wrinkle and crystal boundaries (which trend to be the defective or active spots, as shown in the Figure S10). To eliminate the influence of graphene boundaries in polycrystalline[14] and have a better understanding about the graphene etching process, the etching process was carried out on large size (millimeter size) single-crystal graphene. We adapted previously reported protocol to decrease the nucleation spots on Cu by pre-annealing in H_2-free atmosphere before graphene growth.[15] The experiment was performed almost the same but the Cu heating process was going under 500 sccm Ar atmosphere without H_2. Besides, the single-crystal graphene tends to start etching with higher oxygen concentration than that of polycrystalline graphene as observed in Figure 1. The etching process begins from the center of the hexagonal single crystal graphene (which might be the graphene initial nucleation spot, as shown in Figure S11a-b) by the formation of tiny graphene gaps. It is worth mention that the graphene gaps is of irregular shape, which is different from the regular etched graphene trenches caused by metal particles and SiO_2 particles as reported previously.[16-18] This should be ascribed to the different catalytic activity of oxygen from those particles. As extending growth time, the etching front spreads around by formation of graphene cracks on the graphene surface (Figure S11d), and a series of irregular graphene flakes begin to separate from each other. And then the irregular flakes are further etched and develop into hexagonal graphene fragment (~ 1 μm in size) array structure with edge parallel to each other. This hexagonal graphene fragments are very stable under the high growth temperature, and such structure can be observed after the growth time of 90 h.

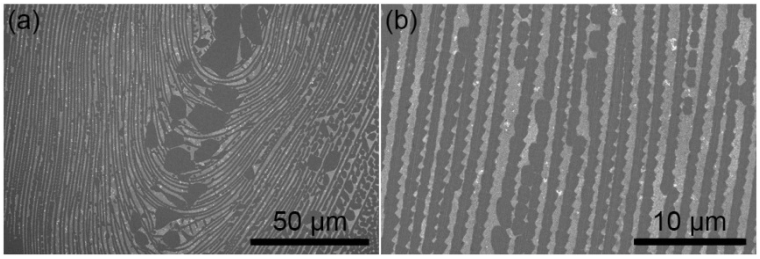

Figure S10. The SEM images of single crystal graphene etching structure forming along with the graphene wrinkles in the growth atmosphere contains 10.8 ppm oxygen for 30 h, respectively.

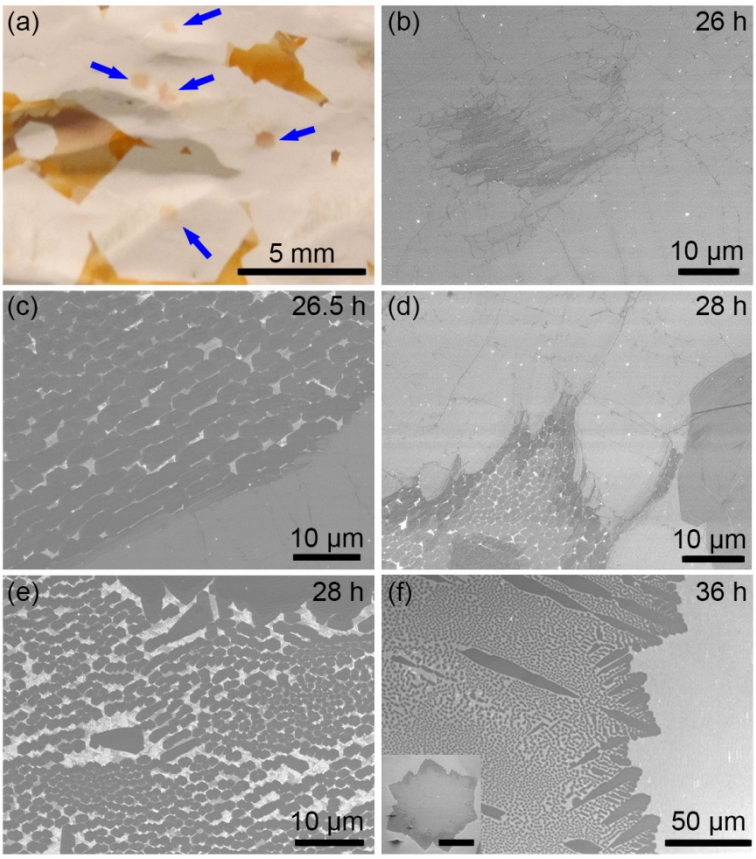

Figure S11. The etching process of single-crystal graphene in the growth atmosphere containing 10.8 ppm oxygen. (a) The optical photograph image of the etched graphene at the initial etching stage with the growth time of 30 h. The Cu foil was pre-heated in air at 200 ˚C for 2 min to make the graphene visible. The etched graphene domains are marked by blue arrows. (b) SEM image of tiny graphene gaps structure. (c) The graphene gaps become greater as time increasing. (d) The boundary between etched graphene zone and intact graphene. (e) The SEM image of irregular graphene flakes. (f) The SEM image of the single-crystal graphene which was thoroughly etched with the growth time of 36h. The insert figure is the large-scale SEM image of the thoroughly etched single-crystal graphene domain, and the scale bar is 500 μm. The graphene growth time in labeled in each SEM image.

The influence of hydrogen on grapheme etching process.

Additionally, during the graphene etching process, we find the graphene etching structure depends on the H_2 concentration during the growth process. As show in Figure S12, the increasing of H_2 concentration can weaken the oxygen etching effect, and on the contrary, the decreasing of H_2 concentration can promote the etching process and results in irregular graphene fragments and faster etching speed. This observation is obviously different from the H_2 etching effect as reported previously.[19]

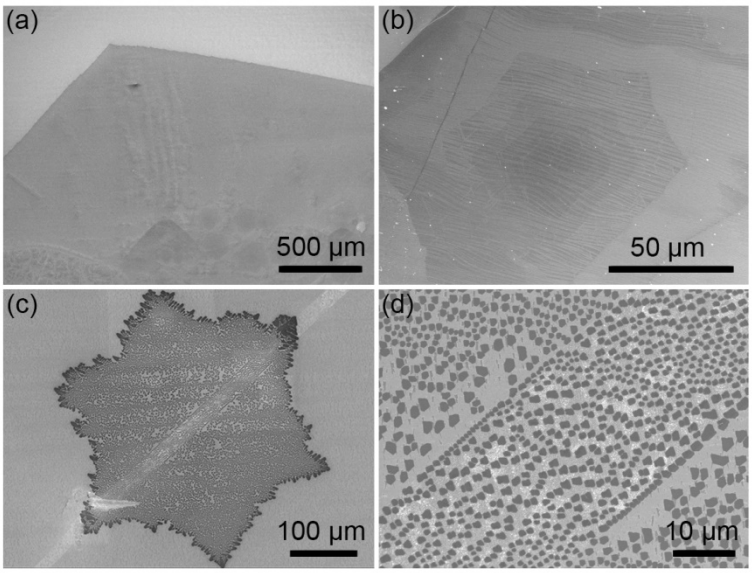

Figure S12. The SEM images of single crystal graphene structure which were grown under different H_2 concentration while with the other growth parameters unchanged. (a-b) The growth was performed in the atmosphere containing 10 sccm H_2 and 10.8 ppm oxygen for 45 h. (c-d) The growth was performed in the atmosphere containing 1.5 sccm H_2 and 10.8 ppm oxygen for 15 h.

REFERENCE

1. J. Li, H. Ji, X. Zhang, X. Wang, Z. Jin, D. Wang and L.-J. Wan, *Chemical Communications*, 2014, **50**, 11012-11015.
2. C. Jia, J. Jiang, L. Gan and X. Guo, *Sci. Rep.*, 2012, **2**.
3. H. Zhou, W. J. Yu, L. Liu, R. Cheng, Y. Chen, X. Huang, Y. Liu, Y. Wang, Y. Huang and X. Duan, *Nat Commun*, 2013, **4**.
4. H.-B. Sun, J. Wu, Y. Han, J.-Y. Wang, F.-Q. Song and J.-G. Wan, *The Journal of Physical Chemistry C*, 2014, **118**, 14655-14661.
5. Z. Sun, A.-R. O. Raji, Y. Zhu, C. Xiang, Z. Yan, C. Kittrell, E. L. G. Samuel and J. M. Tour, *ACS Nano*, 2012, **6**, 9790-9796.
6. L. Liu, H. Zhou, R. Cheng, W. J. Yu, Y. Liu, Y. Chen, J. Shaw, X. Zhong, Y. Huang and X. Duan, *ACS Nano*, 2012, **6**, 8241-8249.
7. X. Zhang, L. Wang, J. Xin, B. I. Yakobson and F. Ding, *Journal of the American Chemical Society*, 2014, **136**, 3040-3047.
8. Y. Wu, H. Chou, H. Ji, Q. Wu, S. Chen, W. Jiang, Y. Hao, J. Kang, Y. Ren, R. D. Piner and R. S. Ruoff, *ACS Nano*, 2012, **6**, 7731-7738.
9. K. Yan, L. Fu, H. Peng and Z. Liu, *Accounts of Chemical Research*, 2013, **46**, 2263-2274.
10. Z. Zhao, Z. Shan, C. Zhang, Q. Li, B. Tian, Z. Huang, W. Lin, X. Chen, H. Ji, W. Zhang and W. Cai, *Small*, 2015, **11**, 1418-1422.

11. P. Wu, X. Zhai, Z. Li and J. Yang, *The Journal of Physical Chemistry C*, 2014, **118**, 6201-6206.
12. G. Ruan, Z. Sun, Z. Peng and J. M. Tour, *ACS Nano*, 2011, **5**, 7601-7607.
13. P. R. Kidambi, B. C. Bayer, R. Blume, Z.-J. Wang, C. Baehtz, R. S. Weatherup, M.-G. Willinger, R. Schloegl and S. Hofmann, *Nano Letters*, 2013, **13**, 4769-4778.
14. A. W. Cummings, D. L. Duong, V. L. Nguyen, D. Van Tuan, J. Kotakoski, J. E. Barrios Vargas, Y. H. Lee and S. Roche, *Advanced Materials*, 2014, **26**, 5079-5094.
15. J. Li, X.-Y. Wang, X.-R. Liu, Z. Jin, D. Wang and L.-J. Wan, *Journal of Materials Chemistry C*, 2015, **3**, 3530-3535.
16. L. C. Campos, V. R. Manfrinato, J. D. Sanchez-Yamagishi, J. Kong and P. Jarillo-Herrero, *Nano Letters*, 2009, **9**, 2600-2604.
17. S. S. Datta, D. R. Strachan, S. M. Khamis and A. T. C. Johnson, *Nano Letters*, 2008, **8**, 1912-1915.
18. L. Gao, W. Ren, B. Liu, Z.-S. Wu, C. Jiang and H.-M. Cheng, *Journal of the American Chemical Society*, 2009, **131**, 13934-13936.
19. I. Vlassiouk, M. Regmi, P. Fulvio, S. Dai, P. Datskos, G. Eres and S. Smirnov, *ACS Nano*, 2011, **5**, 6069-6076.